Biosensors and Bioelectronics 104 (2018) 65–71

Contents lists available at ScienceDirect

Biosensors and Bioelectronics

journal homepage: www.elsevier.com/locate/bios

A novel electrochemiluminescent biosensor based on resonance energy transfer between poly(9,9-di-*n*-octylfluorenyl-2,7-diyl) and 3,4,9,10-perylenetetracar-boxylic acid for insulin detection

Han Zhang[a], Fumei Zuo[a], Xingrong Tan[b], Shenghao Xu[c], Ruo Yuan[a], Shihong Chen[a,*]

[a] Key Laboratory of Luminescence and Real-Time Analytical Chemistry (Southwest University), Ministry of Education, College of Chemistry and Chemical Engineering, Southwest University, Chongqing 400715, PR China

[b] Department of Endocrinology, 9 th People's Hospital of Chongqing, Chongqing 400700, PR China

[c] Key Laboratory of Sensor Analysis of Tumor Marker, Ministry of Education, College of Chemistry and Molecular Engineering, Qingdao University of Science and Technology, Qingdao 266042, PR China

ARTICLE INFO

Keywords:
Insulin
Electrochemiluminescence
Biosensor
PFO
PTCA

ABSTRACT

An electrochemiluminescencent (ECL) biosensor was designed for the determination of insulin using a novel ECL resonance energy transfer (ECL-RET) strategy. In this strategy, carboxyl poly(9,9-dioctyfluorenyl-2,7-diyl) dots (PFO dots) were worked as ECL donor and 3,4,9,10-perylenetetracar-boxylic acid (PTCA) exploited as ECL acceptor, and hydrogen peroxide (H_2O_2) employed as the coreactant. The ECL donor and ECL acceptor were separately labeled with primary antibody (Ab_1) and secondary antibody (Ab_2), forming a sensing interface to the analyte target, insulin. In this expected sandwich-type ECL biosensor, PFO dots acted as sensing platform and PTCA employed as labels to quench the ECL emission of PFO dots. During the determination process, ECL signal of PFO dots was decreased in a gradual way by the increase of insulin concentration, and the quenching mechanism was also investigated. Under the optimal experimental conditions, the constructed biosensor exhibited an excellent performance, including a wide linear range from 1.0×10^{-5} ng/mL to 1.0×10^{2} ng/mL, low detection limit of 3.0×10^{-6} ng/mL, good stability and selectivity for the detection of insulin. This pair of PFO-PTCA, as a new donor-acceptor pair in ECL-RET system, would provide a promising platform for bioanalysis in ECL field.

1. Introduction

Insulin is a peptide hormone, which is produced by beta cells of the pancreatic islets (Arvinte et al., 2010). As one of the important anabolic hormone of human body, insulin can stimulate the glucose in the blood circulation into the liver cells, muscle cells, adipocytes and other tissue cells, thus regulating the metabolism of carbohydrates, fats and protein (Schirhagl et al., 2012; Xiong et al., 2015; Yu et al., 2016). Insulin hormone controls the glucose level in blood within a narrow concentration range and its disorder causes severe illness and dysfunctions in humans which called diabetes mellitus (Abdollah et al., 2007). The sensitive and fast detection of insulin is of great importance because it not only served as a predictor of diabetes of insulinoma and trauma (Melloul et al., 2002) but also was used as a doping drug in competitive sports for cheating (Schirhagl et al., 2012). There have been massive methods employed for the insulin analysis, such as immunoassays (Neal and Han, 2008), high performance liquid chromatography (HPLC) (Mercolini et al., 2008), surface plasmon resonance (Frasconi et al., 2010), electrochemistry (Wang and Li, 2009) and flow injection analysis (Salimi et al., 2009). Among these reported methods, electrochemiluminescence (ECL), as a novel method integrated electrochemistry and luminescence, has arisen growing attention in recent years (Gao et al., 2016). It has been used in DNA, protein and biomolecules analysis and detection due to its high sensitivity, good facility, wide dynamic range, spatial and temporal control and simple instrumentation (Zhang et al., 2017). Thus, it is worth using this kind of excellent potential method for insulin studying.

Due to high sensitivity, non-background unselective photoexcitation and non-interference scattered light, ECL resonance energy transfer (ECL-RET) has drawn wide concern in biosensor field (He et al., 2013; Wu et al., 2014; Dong et al., 2014; Liu et al., 2015). The precondition of ECL-RET is the good spectra overlaps between the energy donors' ECL spectra and the energy acceptors' Uv–vis absorption spectra (Rajapakse et al., 2010; Zhu et al., 2017). While the ECL-RET has been applied into

* Corresponding author.
E-mail address: cshong@swu.edu.cn (S. Chen).

https://doi.org/10.1016/j.bios.2017.12.046
Received 24 September 2017; Received in revised form 20 December 2017; Accepted 26 December 2017
Available online 27 December 2017
0956-5663/

the test of protein (Ji et al., 2014), DNA (Jie et al., 2015) and some ions (Lei et al., 2015), there are still some challenges for searching the corresponding donor-acceptor pair. One of the big challenges is the lack of donor-acceptor system with good spectrum overlap (Ma et al., 2016). Among the reported ECL-RET system, the donor-acceptor pairs are often confined to the following categories, such as quantum dots-Ru $(bpy)_3^{2+}$ (Wu et al., 2012), quantum dots-metal nanoparticles (Zhang et al., 2015), quantum dots-luminol (Zhao et al., 2015), graphene carbonitride (g-C_3N_4)-luminol (Wang et al., 2016) or g-C_3N_4-$Ru(bpy)_3^{2+}$ (Feng et al., 2016a, 2016b). Above donor-acceptor pairs exhibited disadvantages more or less. For example, the quantum dots are commonly poisonous and bad biocompatibility, and the price of $Ru(bpy)_3^{2+}$ is expensive. So, it's significant to exploit efficient, nontoxic and oversimplified ECL-RET system with more types of donor-acceptor collocations.

Conjugated polymers have seen an ongoing interest due to their high fluorescence brightness and excellent photostability, and several views and perspectives about conjugated polymers have been reported in past decades (Wu et al., 2007; Wu and Chiu, 2013). Barbara and his co-workers investigated the ECL behavior of PFBT CPNs for the first time (Chang et al., 2008). Chi and co-workers studied the MEH-PPV CPNs' ECL performance in aqueous solution (Dai et al., 2015). Cheng's group prepared a silole-containing polymer dot, and studied its ECL properties with the coreactant TPrA (Feng et al., 2016a, 2016b). And for our group, we mainly studied poly(9,9-dioctyfluorenyl-2,7-diyl) (PFO). As one of the conjugated polymers, PFO has attracted considerable interest in optoelectronic device, ECL sensors, and other biological labels due to its pleased characters such as high electroluminescence quantum yields with bule light emission, high charge carrier and chemical stability (Zhang et al., 2017). In our previous work, the anodic ECL behavior of PFO was explored in the presence of coreactant $Na_2C_2O_4$. And following we found that H_2O_2 can serve as coreactant to greatly amplify the ECL signal of PFO, thus constructed an oxidase-based biosensor using PFO-H_2O_2 system (Zhang et al., 2017; Chen et al., 2016). We also constructed a ratiometric sensing for detecting organophosphorus pesticides based on carboxyl-PFO dots as anodic luminophore and reduced graphene oxide-CdTe quantum dots as cathodic luminophore (Chen et al., 2017a, 2017b). And all these sensors exhibited a good stability, high sensitivity and excellent selectivity. However, these researches were not mentioning the contents of energy transfer of PFO, and even the application of PFO as energy donor or acceptor. Consequently, investigating the energy transfer performance of PFO was valuable and of great significance since it can extend the application of PFO material in ECL analytical field. Furthermore, it can also expand the range of ECL-RET system, making an addition of energy donor and acceptor pair.

3,4,9,10-perylenetetracar-boxylic acid (PTCA) is the hydrolyzate of perylene-3,4,9,10-tetracarboxylic dianhydride (PTCDA). The ECL properties of perylene derivatives have been studied in recent years in our group. It can be exploited as cathodic luminescent material when worked with the co-reactant $S_2O_8^{2-}$ (Lei et al., 2016), or it worked as the accelerator of coreaction reagent and fixed stabilizer for luminous agent, thus presenting excellent ECL performance (Zhao et al., 2016). However, scanty studies of PTCA was related to the ECL-RET capability. Our group constructed a ratiometric aptasensor based on the energy transfer from peroxydisulfate/oxygen (O_2/$S_2O_8^{2-}$) to amino-terminated perylene derivative (PTC-NH_2). It showed that perylene derivatives such as PTCA may be well employed in ECL-RET system.

Encouraged by the excellent performance of above materials, an ECL biosensor was developed for insulin detection based on the energy transfer from PFO (donor) to PTCA (acceptor). In the present work, PFO dots were connected with the primary of insulin antibody (Ab_1) through the amide bond to synthesize the Ab_1-PFO biocomposites, which then could interact with insulin antigen via specific recognition between antibody and antigen. When the biosensor was modified with PTCA labeled secondary antibody (Ab_2-PTCA), the ECL-RET strategy for detecting insulin was completely achieved. Based on the RET from PFO to PTCA, a series quantitative detection of insulin could be well obtained. In this strategy, a new donor-acceptor pair was investigated, and the absorption spectra of PTCA showed great overlaps with the ECL spectra of synthesized PFO dots. Furthermore, the ECL acceptor PTCA exhibited excellent quenching capability to the ECL donor PFO dots. This new pair of donor-acceptor would extend the ECL-RET system and present their admirable potentiality in further ECL analysis.

2. Experiment

2.1. Reagents and materials

PFO (MW 20000) was provided by ADS Dyes, Inc. (Quebec, Canada). Insulin and insulin antibodies were purchased from Zhengzhou Humanwell Biocell Biotechnology Co. Ltd (Zhengzhou, China). Sigma Chemical Co. (St. Louis, MO, USA) provided the functional copolymer poly(styrene-*co*-maleicanhydride) (PSMA) with MW ~ 1700 and styrene content 68%. N-hydroxysulfosuccinimide (NHS), 1-ethyl-3-[3-(dimethylamino) propyl] carbodiimide hydrochloride (EDC) and bovine serum albumin (BSA) were purchased from Sigma-Aldrich Co. (Shanghai, China). PTCDA and H_2O_2 were provided by Lian Gang Dyestuff Chemical Industry Co. Ltd. (Liaoning, China) and Aladdin Ltd. (Shanghai, China), respectively. Na_2HPO_4 (0.10 M) and KH_2PO_4 (0.10 M) were used to prepare phosphate-buffered saline (PBS, 0.10 M) solutions with various pH. Human serum samples were provided by the 9 th People's Hospital of Chongqing.

2.2. Apparatus

The model MPI-A electro-chemiluminescence analyzer, which was provided by Xi'an Remax Electronic Science & Technology Co. Ltd. (Xi'an, China), was used to perform the ECL measurements. The voltage of photomultiplier tube (PMT) was set at 800 V. The CHI600D electrochemical work station was from Shanghai CH Instruments Co. China, and was used to perform cyclic voltammetry (CV) measurements. Both ECL and CV measurements were carried out using a three-electrode system, which contained a working electrode (modified glassy carbon electrode), a reference electrode (saturated calomel electrode) and a counter electrode (Pt wire). UV–vis absorption spectra and Fourier-transform infrared spectroscopy (FT-IR) were recorded at a UV-2450 UV–VIS Spectrophotometer from Shimadzu Corp. (Tokyo, Japan) and a Nexus 670 FTIR spectrophotometer from Nicolet Instruments (Nicolet Instruments, Tokyo), respectively. The scanning electron microscope (Hitachi, Japan) was used to record scanning electron micrographs (SEM), and the Transmission electron microscopy (TEM) images were obtained from a Hitachi H-800 microscope (Japan).

2.3. Preparation of PFO dots and Ab_1-PFO biocomposite

The carboxyl conjugated PFO dots were obtained according to the literature (Li et al., 2013). First, tetrahydrofuran (THF) was used to dissolve PFO and PSMA to obtain two polymer solutions, respectively. Then, two polymer solutions were blended and diluted with THF. In resultant mixture solution, the concentrations of PFO and PSMA were 50 μg/mL and 10 μg/mL, respectively. Afterwards, under the ultrasonic condition, 1 mL of the mixture solution was added into 1 mL of deionized water. By vacuum evaporation THF was well removed, and after that the carboxyl conjugated PFO dots solution was obtained. Then, insulin Ab_1 was bond to carboxyl group functionalized PFO dots by an EDC/NHS (molar ratio 4:1) coupling protocol and stirred for 6 h, followed by centrifuging to remove unreacted NHS and EDC. 100 μg/mL insulin Ab_1 was mixed with the formed solution and stirred at 4 °C for 24 h. After centrifuging, the resulting Ab_1-PFO was redispersed in pH 7.4 PBS. The obtained dispersion was stored in a refrigerator (4 °C) for further use.

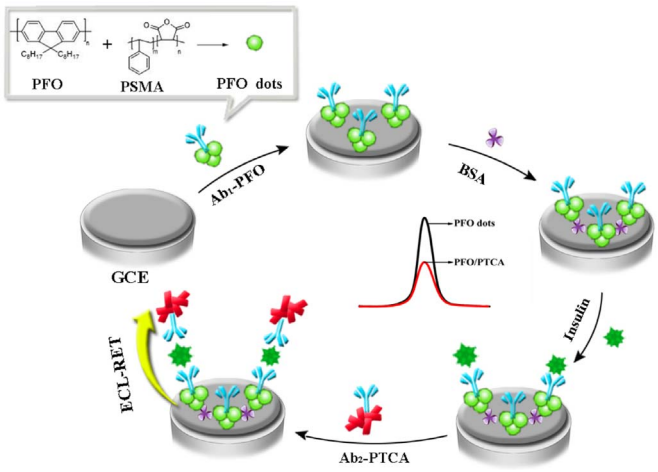

Scheme 1. Schematic description of the fabrication of the ECL biosensor.

2.4. Preparation of Ab_2-PTCA

PTCA was synthesized in accordance with the report (Zhao et al., 2016)]. Firstly, 100 mg PTCDA was hydrolyzed in 20 mL NaOH solution (1.0 M). Afterwards, HCl (1.0 M) was used to make the solution slightly acidic. The resultant PTCA was centrifuged and washed with deionized water for several times. Next, EDC and NHS (molar ratio 4:1) was added to PTCA solution to activate the carboxyl of PTCA under the stirring, followed by adding 100 μg/mL insulin Ab_2 with stirring for a night at 4 °C. After the further purification of Ab_2-PTCA composite was performed through centrifuging and washing with deionized water, it was redispersed in PBS. The obtained dispersion was stored in a refrigerator (4 °C) for further use.

2.5. Fabrication of ECL sensor

Scheme 1 describes the fabrication of the biosensor. Firstly, the bare glassy carbon electrode (Φ = 4.0 mm) was polished with alumina powders (average diameters: 0.3 μm and 0.05 μm) on silk, and then ultrasonically rinsed with ultrapure water and ethanol in turn. After dried in the air, the cleaned GCE was modified with 10 μL of Ab_1-PFO and dried at 4 °C. Afterwards, 1% BSA was used to block nonspecific binding sites of the modified electrode to achieve the biosensor. It was stored in refrigerator before detecting.

2.6. ECL measurement

After the biosensor (Ab_1-PFO/GCE) was incubated with 8 μL of insulin for 2 h, it was further incubated with 10 μL of Ab_2-PTCA at 4 ℃ for 6 h to form the immunocomplex. The ECL measurement was performed in 3 mL PBS (pH 7.4) containing 10 mM H_2O_2 with a scanned potential from 0 to 2 V, and the scan rate was 50 mV/s.

3. Results and discussion

3.1. Characterization of PFO dots and PTCA

The morphologies of PFO dots and PTCA were studied by TEM and SEM, respectively. The corresponding results are displayed in Fig. 1. Fig. 1A was the TEM image of PFO dots, which presented the spherical structure of PFO with the diameter from 60 to 100 nm. The SEM image of PTCA (Fig. 1B) showed an irregularly quadrate-shaped structure, which was consistent with the reported literature (Fu et al., 2017).

PFO dots and PTCA were also characterized by FT-IR spectrum. As shown in Fig. 1C curve a, three character peaks at 3571 cm^{-1}, 1728 cm^{-1} and 722 cm^{-1}, were ascribed to the O-H stretching vibration, C=O stretching vibration and CH=CH bending vibration, respectively. These typical peaks of carboxyl conjugated PFO dots were consist with the literature (Chen et al., 2017a, 2017b), indicating that PFO dots have been successfully obtained. Curve b displayed the following characteristic peaks of PTCA. The absorption peak appeared at 3443 cm^{-1}, which was due to the O-H stretching vibration. The peak at 1773 cm^{-1} was ascribed to the C=O stretching vibration. The typical peak at 1595 cm^{-1} was ascribed to the C=C stretching vibration.

3.2. ECL and CV characterization of the biosensor construction

The stepwise modification process of the biosensor was characterized by ECL measurement in 0.10 M PBS (pH 7.4) containing 10 mM H_2O_2. Fig. 2A displays the corresponding results. As shown, no ECL signal was observed at the bare GCE (curve a). For Ab_1-PFO modified electrode, a strong ECL signal was achieved at 1.98 V (curve b). When BSA (curve c) and insulin solution (curve d) were successively assembled on the electrode, an obviously gradual decrease of ECL intensity was presented. And this phenomenon was due to the obstacle of these nonelectroactive materials. Finally, there was a decline of ECL response for this biosensor when Ab_2-PTCA was immobilized onto the modified electrode (curve e), because an ECL-RET existed between PFO and PTCA, and the PTCA quenched the luminescence of PFO. Above-mentioned changes of the ECL intensity demonstrated that the ECL biosensor was successfully constructed.

The modification procedure of the biosensor was further confirmed by cyclic voltammetry (CV) in 5.0 mM $[Fe(CN)_6^{4-}]/[Fe(CN)_6^{3-}]$ solution at the potential from −0.2 to 0.6 V, and Fig. 2B describes the corresponding results. As seen, the bare electrode presented a well-defined redox peak (curve a). When Ab_1-PFO was incubated onto the electrode, an obviously decreased redox peaks current was observed (curve b). After BSA (curve c) and insulin solution (curve d) were sequentially modified on the electrode, the redox peaks current declined continuously. It was because of the non-conductive properties of BSA and insulin. With the modification of Ab_2-PTCA (curve e), the peak current was also decreased due to the obstacle effect of it.

3.3. Optimization of experimental conditions

Experimental conditions would obviously affect the ECL performance of the constructed biosensor. In order to get good performance for the detection of insulin, the pH of PBS solution and the concentration of H_2O_2 were optimized using Ab_1-PFO/GCE. As described in Fig. 3A, pH influence was investigated, and the maximum ECL response was obtained at pH 7.4. According to the ECL mechanism of PFO-H_2O_2 system (Chen et al., 2016), when the pH ranged from 6.0 to 7.4, with the increase of pH, the concentration of $O_2^{\bullet-}$ in the solution was increased, therefore there would be more excited state PFO*, leading to an increase in ECL signal. When pH exceeded 7.4, the ECL signal decreased with the increase of pH. The reasonable explanation may be as follows. On one hand, at pH 7.4, PFO shows excellent brightness and photostability (Singh et al., 2016). Moreover, the polymer dots exhibit a good fluorescence intensity with PBS (pH 7.4) in the presence of H_2O_2 (Chen et al., 2017a, 2017b; Chan et al., 2011). This may be why the maximum ECL response for Ab_1-PFO/GCE was obtained at pH 7.4. On the other hand, high pH would affect the activity of the antigens and antibodies, further affect the ECL efficiency of PFO and the efficacy of proposed biosensor. In this work, pH 7.4 was chosen as the optimal pH in the further study.

Fig. 3B depicts the effect of the concentration of H_2O_2 on the ECL response of Ab_1-PFO/GCE. As seen, the ECL signal showed a growing trend with the increase of the concentration from 5 mM to 10 mM, and achieved the maximum value at 10 mM H_2O_2. This was due to the massive products of the excited state of PFO. Afterwards, ECL intensity descended as the continuing H_2O_2 concentration increase.

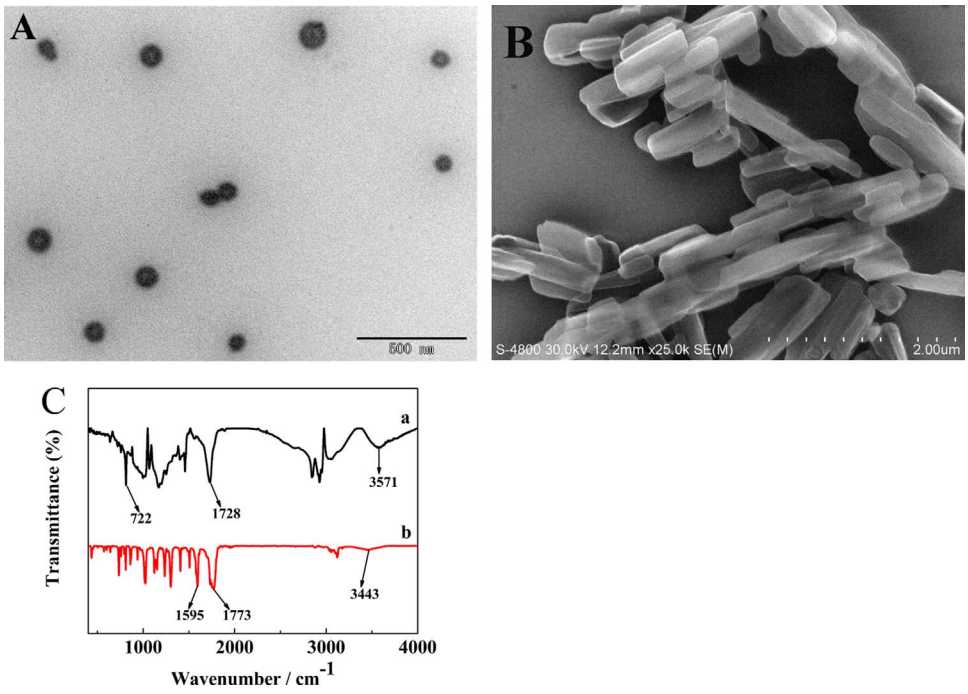

Fig. 1. (A) TEM image of PFO dots; (B) SEM image of PTCA; (C) FT-IR spectra of (a) PFO dots and (b) PTCA.

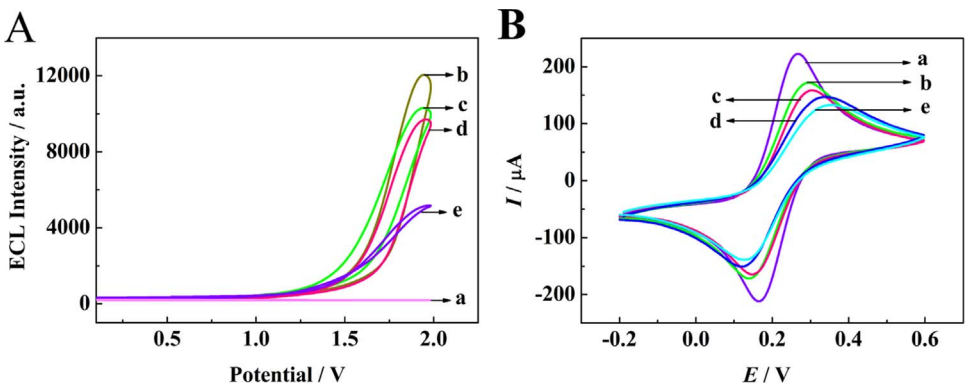

Fig. 2. (A) ECL intensity-potential profiles and (B) CV curves of (a) bare GCE, (b) Ab_1-PFO/GCE, (c) BSA/Ab_1-PFO/GCE, (d) insulin/BSA/Ab_1-PFO/GCE and (e) Ab_2-PTCA/insulin/BSA/Ab_1-PFO/GCE/GCE in 0.10 M PBS (pH 7.4) containing 10 mM H_2O_2 and 5.0 mM $K_3[Fe(CN)_6]/K_4[Fe(CN)_6]$ (1: 1). Scan rate: 50 mV/s.

3.4. Insulin detection of the biosensor

Under the optimal experimental conditions, the detection of insulin was performed at the biosensor, and the results are presented in Fig. 4A. As shown, the increase of insulin concentration induced the decrease of ECL response. It was found that the ECL intensity was logarithmically related to the concentrations of insulin, and a linear range from 1.0×10^{-5} ng/mL to 1.0×10^{2} ng/mL was achieved (Fig. 4B). The detection limit was down to 3.0×10^{-6} ng/mL (S/N = 3), and a linear regression equation $I = -1234.64 \log c + 2737.01$ was obtained with the correlation coefficient 0.9961. This proposed biosensor exhibited a better performance when compared with the previous work (Table 1), including a wider detection range and lower detection limit. The mechanism of this PFO-H_2O_2 system was shown as following (Chen et al., 2016):

$$PFO - e \rightarrow PFO^{\bullet +} \quad (1)$$

$$H_2O_2 \rightarrow HO_2^- + H^+ \quad (2)$$

$$HO_2^- - e \rightarrow HO_2^{\bullet} \quad (3)$$

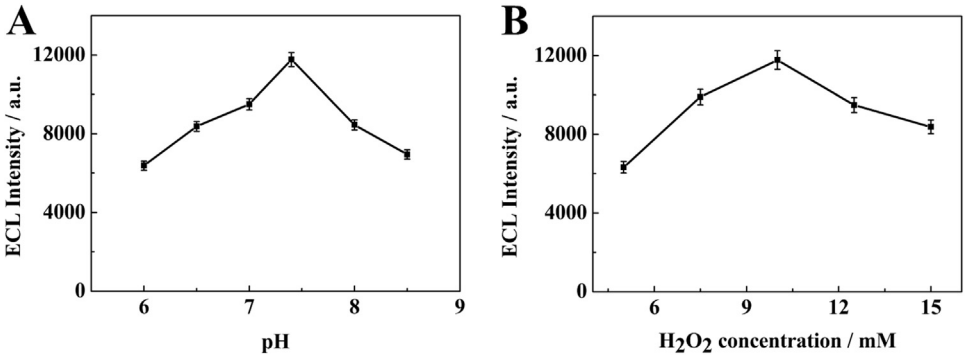

Fig. 3. The effects of (A) pH and (B) concentration of H_2O_2 on the ECL intensity of Ab_1-PFO/GCE.

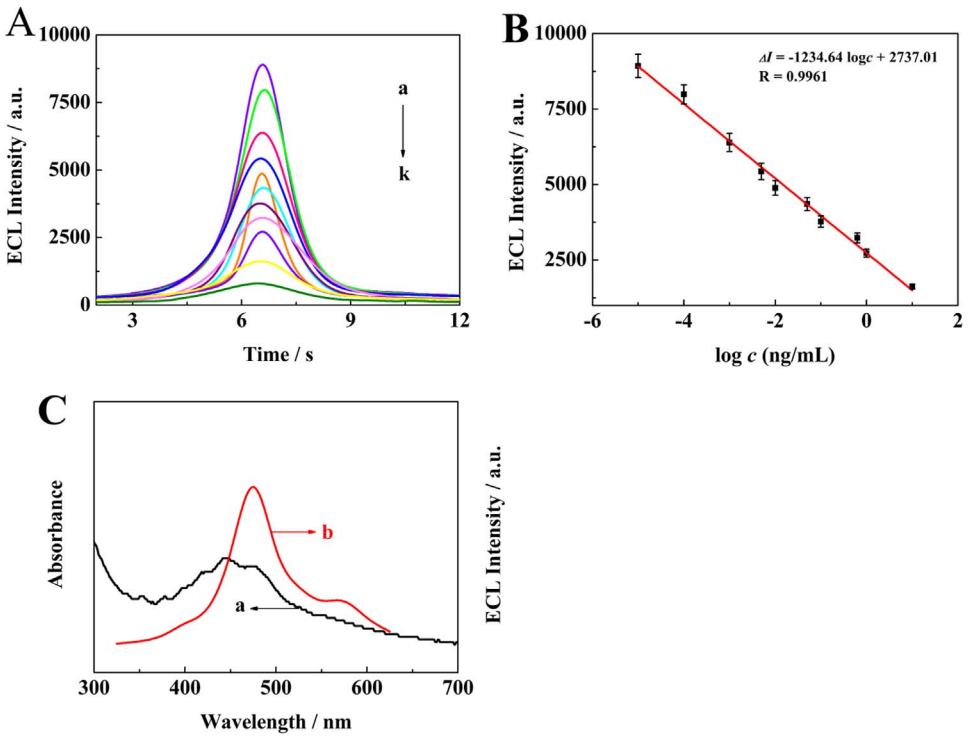

Fig. 4. (A) ECL response of the biosensor to (a) 1.0 × 10^{-5}, (b) 1.0 × 10^{-4}, (c) 5.0 × 10^{-4}, (d) 1.0 × 10^{-3}, (e) 5.0 × 10^{-3}, (f) 1.0 × 10^{-2}, (g) 5.0 × 10^{-2}, (h) 0.1, (i) 1.0, (j)10 and (k) 100 ng/mL insulin in PBS (pH 7.4) containing 10 mM H_2O_2. (B) Calibration curve at different concentration of insulin; (C) UV–vis spectrum of (a) PTCA and ECL spectrum of (b) PFO dots.

Table 1
Analytical performance of different detection approach for the detection of insulin.

Detection method	Linear range	Detection limit	reference
electrochemical detection	100–2400 pM	10 pM	(Yu et al., 2016)
spectroscopic study	2–70 nM	/	(Verdian-Doghaei and Housaindokht, 2015)
fluorescence	4.3–206.4 nM	2.74 nM	(Yang et al., 2018)
photoelectrochemical immunosensor	0.001–20 ng/mL	0.2 pg/mL	(Fan et al., 2017)
ECL	0.1 pg/mL–10 ng/mL	0.042 pg/mL	(Ma et al., 2016)
ECL	10^{-5} ng/mL–100 ng/mL	3 × 10^{-6} ng/mL	this work

$$HO_2^{\bullet} \rightarrow O_2^{\bullet -} + H^+ \quad (4)$$

$$PFO^{\bullet +} + O_2^{\bullet -} \rightarrow PFO^* + O_2 \quad (5)$$

$$PFO^* \rightarrow PFO + h\nu \quad (6)$$

Upon the anodic scan, PFO was firstly oxidized to $PFO^{\bullet +}$. In the presence of H_2O_2, PFO generated an excited state PFO*. Then, excited state PFO* produced a strong intense emission. And as for the quenching mechanism of this system, UV–vis absorption spectrum of PTCA and ECL spectrum of PFO dots have been investigated. As seen from Fig. 4C, there was a good spectra overlaps between the PFO dots' ECL spectra (curve b) and the PTCAs' Uv–vis absorption spectra (curve a), which means that the overlap between emission spectra of PFO dots (donor) and absorption spectra of PTCA (acceptor) enabled the happening of ECL-RET process.

3.5. Analytical performance of ECL biosensor

To investigate the stability of the biosensor, consecutive cyclic potential scans was executed at Ab_2-PTCA/insulin/BSA/Ab_1-PFO/GCE with 1.0 ng/mL insulin in 0.10 M PBS (pH 7.4) containing 10 mM H_2O_2. As seen in Fig. 5A, there was not too much changes among the ECL intensity of these 9 consecutive cycles, and a relatively standard deviation (RSD) of 1.7% was obtained. Additionally, the long-term stability of this biosensor was also studied. As shown in Fig. 5B, after 18 days, the biosensor can retain about 92.1% of its initial response towards 1.0 ng/mL insulin. Above results indicated an acceptable stability of the biosensor.

The selectivity of the proposed biosensor was further evaluated using common interfering substances, including BSA, alpha-fetoprotein (AFP), carcinoembryonic antigen (CEA) and human serum albumin (HSA). These interfering substances were added into 1.0 ng/mL insulin solution for the investigation. And the corresponding results were depicted in Fig. 5C, and it could be observed that there was not much differences among these data. Negligible interference from above interfering substances demonstrated an excellent selectivity of the constructed biosensor.

Additionally, the reproducibility was also studied using 5 developed biosensors incubated with the same concentration insulin solution (1.0 ng/mL) under the same optimal conditions. The RSD of measurements was 3.7%, indicating an acceptable reproducibility.

3.6. Insulin detection in human serum samples

The human serum samples obtained from the local hospital were chosen to investigate the potential applicability of the proposed ECL biosensor. On the one hand, three human serum samples, which were diluted by the PBS solution (pH 7.4) into 2-fold diluted solutions, were detected using our proposed biosensor and the detection results were compared with those from the hospital official method (Table 2). The relative errors (±) between our ECL method and the hospital official method were calculated using the formula $E_r = \frac{\bar{x} - x_T}{x_T} \times 100\%$. Here, $\bar{x}$ means the average concentration of the detection results for three times by our proposed ECL biosensor, and x_T means the value from the hospital official method. The relative errors in the range of −4.9% ~ +7.2% were obtained (Table 2), which showed that the results from our ECL method exhibited a good consistency with those form the hospital method. On the other hand, the Sample 3 was diluted by the

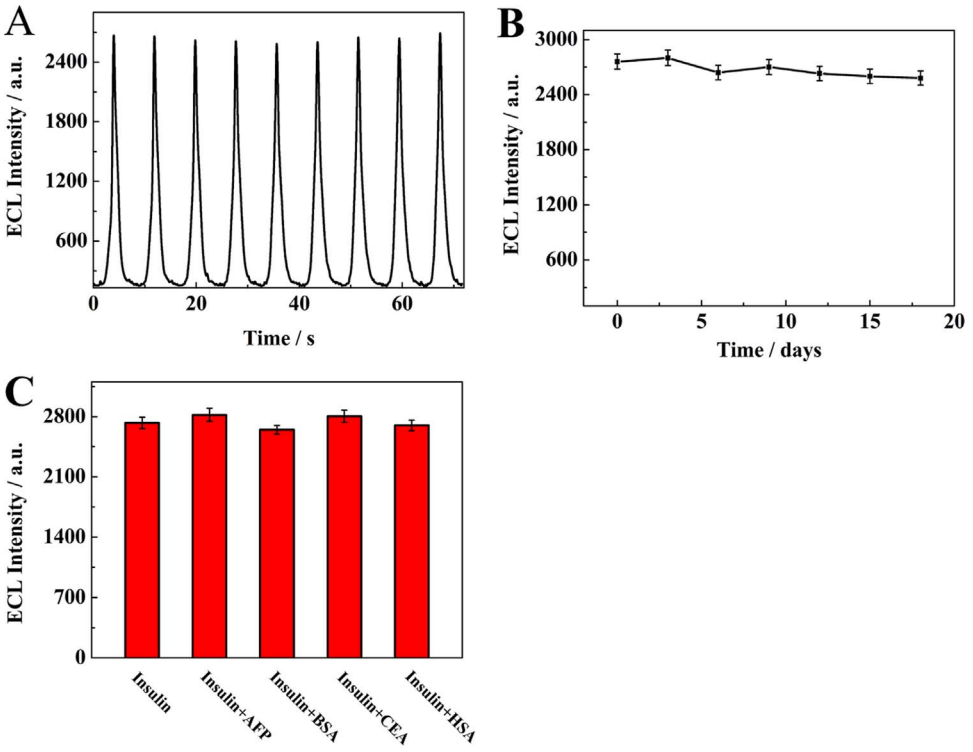

Fig. 5. (A) The ECL stability and (B) Long-term stability of the biosensor for the detection of 1.0 ng/mL insulin; (C) ECL response of the biosensor incubated in (a) insulin (1.0 ng/mL), (b) insulin (1.0 ng/mL) + AFP (100 ng/mL), (c) insulin (1.0 ng/mL) + BSA (100 ng/mL), (d) insulin(1.0 ng/mL) + CEA (100 ng/mL) and (e) insulin (1.0 ng/mL) HSA (100 ng/mL).

Table 2
Comparison between hospital detection and ECL method.

Samples	Hospital detection (ng/mL)	ECL[a] (ng/mL)	E_r (%)
1	6.70×10^{-5}	$(6.37 \pm 0.23) \times 10^{-5}$	−4.9
2	9.60×10^{-5}	$(10.21 \pm 0.31) \times 10^{-5}$	+6.4
3	4.30×10^{-5}	$(4.61 \pm 0.11) \times 10^{-5}$	+7.2

[a] Mean ± *SD*, $n = 3$.

Table 3
Recoveries of insulin in diluted human serum samples.

Samples	Original found (ng/mL)	Added (ng/mL)	Found[a] (ng/mL)	Recovery (%)
3-1	2.15×10^{-4}	1.00×10^{-4}	$(3.16 \pm 0.06) \times 10^{-4}$	101
3-2	2.15×10^{-4}	1.00×10^{-3}	$(1.18 \pm 0.04) \times 10^{-3}$	97
3-3	2.15×10^{-4}	1.00×10^{-2}	$(1.00 \pm 0.05) \times 10^{-2}$	98
3-4	2.15×10^{-4}	1.00	0.97 ± 0.03	97
3-5	2.15×10^{-4}	10.0	10.3 ± 0.05	103

[a] Mean ± *SD*, $n = 3$.

PBS solution (pH 7.4) into 2-fold diluted human serum samples to perform the recovery experiments using standard addition method. Table 3 presents the corresponding results, and the recoveries ranged from 97% to 103%. The results in Tables 2 and 3 were detected for three times and presented as Mean ± *SD* (Mean and *SD* represent the average concentration of insulin and the standard deviation, respectively). Above experiments indicated that our constructed biosensor exhibited an acceptable accuracy and has a promising application for detecting real biological samples.

4. Conclusion

In summary, we synthesized carboxyl poly(9,9-dioctyfluorenyl-2,7-diyl) dots (PFO dots) and 3,4,9,10-perylenetetracar-boxylic acid (PTCA) to form a new ECL-RET system for the sensitive detection of insulin. In the proposed system, PFO dots worked as the energy donor and PTCA employed as the energy acceptor. In the presence of coreactant H_2O_2, PFO dots showed a high ECL intensity. Additionally, the ECL emission of PFO dots could be effectively quenched by PTCA, and the quenching mechanism was also investigated. Furthermore, the constructed biosensor presented excellent performance, including a wide linear range, low detection limitation, good stability and selectivity for insulin detection. This new donor-acceptor pair would expand the ECL-RET system and exhibit an enviable potential in further ECL analysis. Moreover, PTCA may be able to combine with other luminescent materials to form more ECL-RET systems for bioanalysis.

Acknowledgments

This work was supported by National Natural Science Foundation of China (21775122, 21775123, 21775124, 51473136, 21575116), Medical Scientific Research Projects of Health Bureau of Chongqing (2016ZDXM039, 2017ZBXM018) and Fundamental Research Funds for the Central Universities (XDJK2017A001), China.

References

Abdollah, S., Mahmoud, R., Saied, S., Rahman, H., 2007. Anal. Chem. 79, 7431–7438.
Arvinte, A., Westermann, A.C., Sesay, A.M., Virtanen, V., 2010. Sens. Actuator B: Chem. 150, 756–763.
Chan, Y.H., Wu, C.F., Ye, F.M., Jin, Y.H., Smith, P.B., Chiu, D.T., 2011. Anal. Chem. 83, 1448–1455.
Chang, Y.L., Palacios, R.E., Fan, F.R.F., Bard, A.J., Barbara, P.F., 2008. J. Am. Chem. Soc. 28, 8906–8907.
Chen, H.M., Lu, Q.Y., Liao, J.Y., Yuan, R., Chen, S.H., 2016. Chem. Commun. 52, 7276–7279.
Chen, H.M., Zhang, H., Yuan, R., Chen, S.H., 2017a. Anal. Chem. 89, 2823–2829.
Chen, L., Wu, L., Yu, J., Kuo, C.T., Jian, T., Wu, I.C., Rong, Y., Chiu, D.T., 2017b. Chem. Sci. 8, 7236–7245.
Dai, R., Wu, F., Xu, H., Chi, Y., 2015. ACS Appl. Mater. Interfaces 28, 15160–15167.
Dong, Y.P., Gao, T.T., Zhou, Y., Zhu, J.J., 2014. Anal. Chem. 86, 11373–11379.
Fan, D.W., Wang, H.Y., Khan, M.S., Bao, C.Z., Wang, H., Wu, D., Wei, Q., Du, B., 2017. Biosens. Bioelectron. 97, 253–259.
Feng, Q.M., Shen, Y.Z., Li, M.X., Zhang, Z.L., Zhao, W., Xu, J.J., Chen, H.Y., 2016a. Anal.

Chem. 88, 937–944.
Feng, Y.Q., Dai, C.H., Lei, J.P., Ju, H.X., Cheng, Y.X., 2016b. Anal. Chem. 88, 845–850.
Frasconi, M., Tortolini, C., Botre, F., Mazzei, F., 2010. Anal. Chem. 82, 7335–7342.
Fu, X.M., Yang, Y., Wang, N., Chen, S.H., 2017. Sens. Actuator B: Chem. 250, 584–590.
Gao, W.Y., Liu, Z.Y., Qi, L.M., Lai, J.P., Kitte, S.A., Xu, G.B., 2016. Anal. Chem. 88, 7654–7659.
He, L.J., Wu, M.S., Xu, J.J., Chen, H.Y., 2013. Chem. Commun. 49, 1539–1541.
Ji, J., He, L., Shen, Y.Y., Hu, P.P., Li, X.H., Jiang, L.P., Zhang, J.R., Li, L.L., Zhu, J.J., 2014. Anal. Chem. 86, 3284–3290.
Jie, G.F., Qin, Y.Q., Meng, Q.M., Wang, J.L., 2015. Analyst 140, 79–82.
Lei, Y.M., Huang, W.X., Zhao, M., Chai, Y.Q., Yuan, R., Zhuo, Y., 2015. Anal. Chem. 87, 7787–7794.
Lei, Y.M., Zhao, M., Wang, A., Yu, Y.Q., Chai, Y.Q., Yuan, R., Zhuo, Y., 2016. Eur. J. 22, 8207–8214.
Li, Q., Sun, K., Chang, K.W., Yu, J.B., Chiu, D.T., Wu, C.F., Qin, W.P., 2013. Anal. Chem. 85, 9087–9091.
Liu, Z.Y., Qi, W.J., Xu, G.B., 2015. Chem. Soc. Rev. 44, 3117–3142.
Ma, H.M., Li, X.J., Yan, T., Li, Y., Liu, H.Y., Zhang, Y., Wu, D., Du, B., Wei, Q., 2016. ACS Appl. Mater. Interfaces 8, 10121–10127.
Melloul, D., Marshak, S., Cerasi, E., 2002. Diabetologia 45, 309–326.
Mercolini, L., Musenga, A., Saladini, B., Bigucci, F., Luppi, B., Zecchi, V., Raggi, M.A., 2008. J. Pharm. Biomed. Anal. 48, 1303–1309.
Neal, J., Han, W., 2008. Endocr. Pract. 14, 1006–1010.
Rajapakse, H.E., Gahlaut, N., Mohandessi, S., Yu, D., Turner, J.R., Miller, L.W., 2010. Proc. Natl. Acad. Sci. USA 107, 13582–13587.
Salimi, A., Mohamadi, L., Hallaj, R., Soltanian, S., 2009. Electrochem. Commun. 11, 1116–1119.
Schirhagl, R., Latif, U., Podlipna, D., Blumenstock, H., Dickert, F.L., 2012. Anal. Chem. 84, 3908–3913.
Singh, A., Bezuidenhout, M., Walsh, N., Beirne, J., Felletti1, R., Wang, S.,X., Fitzgerald, K.,T., Gallagher, W.,M., Kiely, Patrick, Redmond, G., 2016. Nanotechnology 27, 305603.
Verdian-Doghaei, A., Housaindokht, M.R., 2015. J. Lumin. 159, 1–8.
Wang, Y.Z., Hao, N., Feng, Q.M., Shi, H.W., Xu, J.J., Chen, H.Y., 2016. Biosens. Bioelectron. 77, 76–82.
Wang, Y., Li, J., 2009. Anal. Chim. Acta 650, 49–53.
Wu, C.F., Chiu, D.T., 2013. Angew. Chem. Int. Ed. 52, 3086–3109.
Wu, C.F., Szymanski, C., Cain, Z., McNeill, J., 2007. J. Am. Chem. Soc. 129, 12904–12905.
Wu, M.S., He, L.J., Xu, J.J., Chen, H.Y., 2014. Anal. Chem. 86, 4559–4565.
Wu, M.S., Shi, H.W., He, L.J., Xu, J.J., Chen, H.Y., 2012. Anal. Chem. 84, 4207–4213.
Xiong, Y., Deng, C., Zhang, X., Yang, P., 2015. ACS Appl. Mater. Interfaces 7, 8451–8456.
Yang, J.J., Zhang, Z.F., Yan, G.Q., 2018. Sens. Actuator B: Chem. 255, 2339–2346.
Yu, Y., Guo, M., Yuan, M., Liu, W., Hu, J., 2016. Biosens. Bioelectron. 77, 215–219.
Zhang, H., Lu, Q.Y., Zuo, F.M., Yuan, R., Chen, S.H., 2017. Sens. Actuator B: Chem. 241, 887–894.
Zhang, Y.Y., Feng, Q.M., Xu, J.J., Chen, H.Y., 2015. ACS Appl. Mater. Interfaces 47, 26307–26314.
Zhao, H.F., Liang, R.P., Wang, J.W., Qiu, J.D., 2015. Chem. Commun. 51, 12669–12672.
Zhao, J., Lei, Y.M., Chai, Y.Q., Yuan, R., Zhuo, Y., 2016. Biosens. Bioelectron. 86, 720–727.
Zhu, W.J., Wang, C., Li, X.J., Khan, M.S., Sun, X., Ma, H.M., Fan, D.W., Wei, Q., 2017. Biosens. Bioelectron. 97, 115–121.